

RND pumps across the genus *Acinetobacter*: AdelJK is the universal efflux pump

Elizabeth M. Darby¹, Vassilij N. Bavro², Steven Dunn¹, Alan McNally¹ and Jessica M. A. Blair^{1*}

Abstract

Acinetobacter are generally soil-dwelling organisms that can also cause serious human infections. *A. baumannii* is one of the most common causative agents of *Acinetobacter* infections and is often multidrug resistant. However, an additional 25 species within the genus have also been associated with infection. *A. baumannii* encodes six resistance nodulation division (RND) efflux pumps, the most clinically relevant class of efflux pumps for antibiotic export, but the distribution and types of RND efflux pumps across the genus is currently unknown. Sixty-four species making up the genus *Acinetobacter* were searched for RND systems within their genomes. We also developed a novel method using conserved RND residues to predict the total number of RND proteins including currently undescribed RND pump proteins. The total number of RND proteins differed both within a species and across the genus. Species associated with infection tended to encode more pumps. AdelJK/AdeXYZ was found in all searched species of *Acinetobacter*, and through genomic, structural and phenotypic work we show that these genes are actually homologues of the same system. This interpretation is further supported by structural analysis of the potential drug-binding determinants of the associated RND-transporters, which reveal their close similarity to each other, and distinctiveness from other RND-pumps in *Acinetobacter*, such as AdeB. Therefore, we conclude that AdelJK is the fundamental RND system for species in the genus *Acinetobacter*. AdelJK can export a broad range of antibiotics and provides crucial functions within the cell, for example lipid modulation of the cell membrane, and therefore it is likely that all *Acinetobacter* require AdelJK for survival and homeostasis. In contrast, additional RND systems, such as AdeABC and AdeFGH, were only found in a subset of *Acinetobacter* that are associated with infection. By understanding the roles and mechanisms of RND efflux systems in *Acinetobacter*, treatments for infections can avoid efflux-mediated resistance and improve patient outcomes.

DATA SUMMARY

This study made use of publicly available datasets downloaded from NCBI's GenBank. A full list of accession numbers can be found in Supplementary S3 text 3 (available in the online version of this article). Bioinformatics software used in this study was previously published and is listed in the Methods section. The BLASTp conserved residue files are in Supplementary S3 text 1 and 2.

INTRODUCTION

Members of the genus *Acinetobacter* are Gram-negative bacteria commonly isolated from soil and water [1]. However, many species are also important human pathogens and *Acinetobacter baumannii* is on the World Health Organisation's priority pathogens list due to the number of drug-resistant infections it causes [2]. In addition to *A. baumannii*, a number of other *Acinetobacter* species are known to cause human infections, for example *A. lwoffii*, which is the leading cause of *Acinetobacter*-derived bacteraemia in England, and *A. nosocomialis* and *A. pittii*, which also cause nosocomial infections [3, 4].

Received 19 October 2022; Accepted 19 January 2023; Published 30 March 2023

Author affiliations: ¹Institute of Microbiology and Infection, University of Birmingham, Edgbaston, Birmingham, B15 2TT, UK; ²School of Life Sciences, University of Essex, Colchester, CO4 3SQ, UK.

***Correspondence:** Jessica M. A. Blair, j.m.a.blair@bham.ac.uk

Keywords: *Acinetobacter*; antibiotic resistance; efflux; RND.

Abbreviations: DBP, distal binding pocket; HAE, hydrophobic and amphiphilic efflux; HME, heavy metal efflux; MDR, multi-drug resistance; MIC, minimum inhibitory concentration; OMF, outer membrane factor; PAP, periplasmic adaptor protein; PBP, Proximal Binding Pocket; RND, resistance nodulation division.

Data statement: All supporting data, code and protocols have been provided within the article or through supplementary data files. Supplementary material is available with the online version of this article.

000964 © 2023 The Authors



This is an open-access article distributed under the terms of the Creative Commons Attribution NonCommercial License. This article was made open access via a Publish and Read agreement between the Microbiology Society and the corresponding author's institution.

Impact Statement

Efflux pumps extrude antibiotics from within bacterial cells, directly conferring antibiotic resistance and underpinning other mechanisms of resistance. By understanding the exact complement of efflux pumps and their roles across infection-causing organisms such as those within the genus *Acinetobacter*, it is possible to understand how cells become resistant to antibiotics and how this might be tackled. Efflux is an attractive target for inhibition to increase susceptibility to existing drugs and, therefore, knowing which pumps are present in each species is important. Furthermore, we present a novel method using conserved resistance nodulation division (RND) residues to predict the total number of RND proteins including currently novel systems, within bacterial genomes.

A. baumannii isolates are commonly multidrug resistant and this is mediated by a combination of molecular mechanisms including acquired resistance genes (e.g. *bla*_{OXA-23}) [5], mutations in genes encoding the target of antibiotics, for example *gyrA* [6], and increased expression of multidrug efflux pump systems which actively pump antibiotic compounds out of the cell [7, 8] and allow the cell time to evolve other mechanisms of resistance [9]. Of particular importance are efflux pumps from the resistance nodulation division (RND) family. RND systems are broadly split into two categories based upon the substrates they export – hydrophobic and amphiphilic efflux pumps (HAE) which contribute to antimicrobial resistance and heavy metal efflux pumps (HME) [10]. Typical RND systems are tripartite efflux pumps, which are built around an inner membrane H⁺/drug antiporter [10] called the RND transporter, the allosteric ‘pumping’ of which allows the drug to be acquired from either the periplasmic space or the outer leaflet of the inner membrane and passed out of the cell via a conduit involving the partner outer membrane factor (OMF) channels that span the outer membrane and periplasmic adaptor proteins (PAPs) that connect the RND transporter and OMF channels [11–14]. The RND transporters themselves function as trimers, which contain three functionally interdependent protomers, cycling consecutively through the Loose (L), Tight (T) and Open (O) conformational states during cooperative catalysis [15, 16]. RND pumps exhibit a broad substrate specificity which is underpinned by the presence of distinct binding pockets within the transporter protomers. The principal binding pockets are known as the ‘Proximal Binding Pocket’ (PBP) and ‘Distal Binding Pocket’ (DBP), which have wide specificities, but are broadly associated with the processing of drugs of different molecular weight and are separated by the so-called gating- or switch-loop [15, 17–19].

To date, nine RND transporter genes have been found in *Acinetobacter*: *adeJ*, *adeB*, *adeE*, *adeG*, *adeY*, *abeD*, *arpB*, *acrB* and *czcA* [7, 20–28]. AdeABC, AdeFGH and AdeIJK have all been characterized in *A. baumannii* and are known to export a broad range of compounds. AdeABC exports aminoglycosides, trimethoprim, chloramphenicol and fluoroquinolones [20, 21]. AdeFGH also exports trimethoprim, chloramphenicol and fluoroquinolones, but in addition exports tetracycline, tigecycline and clindamycin [7]. Lastly, AdeIJK exports chloramphenicol, tetracycline, fluoroquinolones, trimethoprim as well as beta lactams, erythromycin, lincosamides, fusidic acid, novobiocin and rifampicin [23]. Expression of AdeABC and AdeFGH can be increased in the presence of an antibiotic challenge, leading to reduced susceptibility to the drug [7, 29, 30]. AdeIJK is constitutively expressed and provides intrinsic levels of resistance to antibiotics. Whilst small increases in expression have been characterized, leading to multi-drug resistance (MDR) phenotypes, increased expression of AdeIJK can be toxic to the cell, and therefore increased expression of AdeABC and AdeFGH more commonly mediate MDR [31, 32].

The number of RND efflux pumps present varies between bacterial species and also within members of the same species [11, 14, 24, 33, 34]. For example, *Neisseria gonorrhoeae* has only one RND system, while *Pseudomonas aeruginosa* can have up to 12, showing that the number of RND genes in a given genome does not necessarily correlate with the ability of bacteria to cause human infections [14]. However, it seems plausible that encoding more RND systems may allow a bacterium to adapt to a broader range of environmental stresses.

While a number of efflux pumps have been well studied in *A. baumannii*, the range of RND systems across the genus *Acinetobacter* is not currently known. In this study we have developed a method to search available genomes for RND efflux systems and have used it to determine their number, type and distribution across the entire genus *Acinetobacter*, and have considered whether these correlate with species that commonly cause human infections. By mapping these data onto the phylogeny of the genus *Acinetobacter*, combined with structural modelling of these systems, we have shown that the pumps currently annotated as AdeIJK and AdeXYZ are actually homologous RND systems, forming a distinct clade from other Gram-negative RND systems. In addition, we show that AdeIJK is the ancestral pump found across all *Acinetobacter* species and that other RND systems, such as AdeABC, have been acquired independently in specific *Acinetobacter* species.

METHODS**Predicting the total number of RND transporter proteins within a whole genome sequence**

Amino acid sequences of characterized HAE proteins from 15 different Gram-negative bacterial species and HME RND proteins from seven different species were aligned in separate files using MAFFT (v.7) [35]. Alignments of the final HAE and HME

transporter proteins used can be found in Supplementary S1, Figs S1 and S2. The consensus sequence in >80% of the aligned sequences was taken from either alignment file to create conserved residue files, Supplementary S3, texts S1–2, which can then be searched using BLASTp for other RND pump proteins encoded in genomes from both *Acinetobacter* and other Gram-negative species [36]. Specifically, the genome .fasta files (which included both chromosomal and plasmid contigs) were downloaded and subsequently annotated using Prokka (v.1.14.6) [37]. The .faa output files were concatenated into a single file which was made into a BLASTp protein database (makeblastdb) to search for HAE/HME pump proteins. An e-value cutoff of 10 was used for BLASTp on the command line to highlight divergent RND proteins.

For the prediction of RND transporter proteins across the genus, up to four reference sequences per *Acinetobacter* species were downloaded from NCBI, totalling 170 genomes. A full list of sequences and accession codes can be found in Supplementary S2, Table S1. At the time of analysis there were 64 *Acinetobacter* species fully validated by the International Code of Nomenclature of Prokaryotes (ICNP) (<https://lpsn.dsmz.de/genus/acinetobacter>).

When determining the number of RND proteins in other Gram-negative species the following reference sequences were searched: *A. baumannii* ACICU NC_010611.1, *A. baumannii* AYE NC_010410.1, *C. jejuni* NCTC 11168 GCF_900475265.1, *E. coli* K12 MG1655 NC_000913.3, *H. influenzae* NCTC 8143 GCF_001457655.1, *K. pneumoniae* ATCC 43816 NZ_CP064352.1, *N. gonorrhoeae* FA1090 NC_002946.2, *P. aeruginosa* PAO1 GCF_000006765.1, *Salmonella enterica* SL1344 NC_016810.1 and *Shigella flexneri* 5a M90T NZ_CP037923.1.

Furthermore, 100 *A. baumannii* assemblies from NCBI were downloaded to determine if the number of RND proteins differs within a species (Supplementary S3, text S3). These assemblies were quality checked using Quast (v.5.0.2) [38], where all assemblies had an N50 of >30 000. Furthermore, their average nucleotide identity across the genome compared to *A. baumannii* AYE (NC_010410.1) was confirmed to be >95% using fastANI (v.1.31) [39]. The presence of duplicate *A. baumannii* genomes was detected using MASH (v.2.2.2) to confirm all genomes represented genetically distinct strains [40]. The same sequences were used for recombination analysis of AdeABC, AdeFGH and AdeIJK (see below).

Finding individual known RND genes across *Acinetobacter*

In addition to searching for the number of RND pump proteins encoded in the genomes, the presence of known RND genes was also determined across the entire genus. The sequences of RND genes were searched using ABRicate (v.0.8.13) with a custom database consisting of PAP, RND and OMF encoding genes (S3 text S4) [41]. Most reference gene sequences were from *A. baumannii* AYE (NC_010410.1), apart from *adeDE* from *A. pittii* PHEA-2 (NC_016603.1), *adeXYZ* from *A. baylyi* ADP1 (NC_005966.1) and *acrAB* from *A. nosocomialis* NCTC 8102 (NZ_CP029351.1). ABRicate cut-off values of >50% identity and >50% coverage were used to highlight homologues in the different species with divergent nucleic acid sequences.

The heatmap displaying the number of RND transporter proteins and presence of RND genes was created using the R packages gheatmap in ggtree, ggplot2 and treeio, where the phylogenetic tree and the metadata were visualized [42–45]. A literature search was done to determine if a given *Acinetobacter* species had been documented to cause human infection by searching PubMed for the given species and ‘infection’. The phylogenetic tree of *Acinetobacter* was created using a core gene alignment generated by Panaroo (v.1.2.3) as an input for Fasttree (v.2.1.10) [46] and mid-point rooted. Fasttree was implemented using the generalized time reversible model of evolution [47]. To investigate if the number of RND proteins was correlated with the ability to cause human infection, a point biserial Pearson’s correlation was conducted using SPSS (IBM) (v.28) [48].

Genomic context and recombination

To determine if *adeIJK* is found in the same genomic context in three species of *Acinetobacter*, *A. baumannii* AYE (NC_010410.1), *A. lwoffii* 5867 (GCA_900444925.1) and *A. baylyi* ADP1 (NC_005966.1), 10 kb of sequence up- and downstream of *adeIJK* was extracted and visualized in Easyfig (v.2.2.5), with tBLASTx homology annotated [36, 49]. To assess whether *adeABC*, *adeFGH* or *adeIJK* were found in a recombination hotspots, whole genome alignments of *A. baumannii* ($n=100$ assemblies, described above, mapped against the *A. baumannii* AYE NC_010410.1 reference) were created using Snippy (4.6.0) and Gubbins (v.3.1.3), where Gubbins highlighted areas of recombination [50, 51]. Recombination predictions were visualized in Phandango [52].

Structural analysis and modelling of *Acinetobacter* RND pump components

A phylogenetic tree to show that AdeJ/AdeY cluster together, separate from other RND proteins, was created using a MAFFT (v.7) alignment of RND proteins from Gram-negative species (those used for the BLASTp conserved residue alignment), including multiple copies of AdeJ and AdeY from distantly related *Acinetobacter* species. The tree was created using phylo.io in MAFFT (Neighbour joining, JTT model, 100 bootstraps) and edited in iTol (v.5) [35, 53]. Experimental structures of AdeJ from *A. baumannii* in both apo- and eravacycline-bound forms (7M4Q.pdb and 7M4P.pdb respectively [54]) were used to perform homology modelling of AdeJ from *A. lwoffii* (76.38% identity) and AdeY from *A. baylyi* (79.25% identity), using I-TASSER [55].

For analysis of the properties of the drug-binding pockets, the experimental eravacycline-bound structure of *A. baumannii* AdeJ (PDB ID 7M4P, chain B), corresponding to the T-conformer, was used, as well as the corresponding T-conformer structures of AcrB occupied by minocycline (PDB ID 4D×5.pdb, chain B [56]) and levofloxacin (PDB ID 7B8T, chain C [57]). In addition, the L-conformer of the asymmetric AcrB (4D×5.pdb [56]) and the L-conformer of the AdeB in L*OO state (7B8Q.pdb [57]) were used to analyse the drug-binding pockets of AcrB and AdeB respectively, alongside the L-conformer and the ampicillin-bound T-conformer of the MtrD structure (6VKS.pdb [58]). Sequence alignments were performed with MAFFT (v.7) [35], and secondary structure was visualized with ESript 3 [59]. All visualizations were done with the PyMOL Molecular Graphics System (v.1.8; Schrödinger, LLC).

Cloning of *Acinetobacter* efflux genes

Efflux pump genes *adeIJK* from *A. baumannii* AYE and *adeXYZ* from *A. baylyi* ADP1 (Supplementary S2, Table S2) were cloned using NEB HiFi cloning (New England Biolabs) into the expression vector pVRL2 [60]. Briefly, the efflux genes were amplified using PCR and primers in Supplementary S2, table S3. The vectors were digested using *NotI*-HF and *XmaI* restriction endonucleases (New England Biolabs) that left complementary overhangs to the PCR products. The PCR products and digested vectors were then ligated using HiFi assembly mix. Cloned vectors were electroporated (2.5 kV, 5 µF, 200 Ω) into cold electrocompetent *A. baumannii* ATCC 17978 UN [61] Δ *adeAB* Δ *adeFGH* Δ *adeIJK* to determine function. Electrocompetent cells were made as described previously [62]. The complete sequence of cloned vectors was determined by Plasmidsaurus (sequencing files in Supplementary files S5 and S6) [63].

Antimicrobial susceptibility

The minimum inhibitory concentration was measured using a broth micro-dilution method according to CLSI guidance with 1% arabinose (Acros Organics) [64, 65]. Compounds were chosen because they are exported by different Ade systems: ampicillin (Sigma), chloramphenicol (Sigma), ciprofloxacin (Acros Organics), clindamycin hydrochloride (TCI Chemicals), ethidium bromide (Acros Organics), rifampicin (Fisher) and tetracycline (Sigma).

RESULTS

Novel search using RND consensus sequences to detect HAE and HME pump proteins

The number of inner membrane RND pump proteins is known to differ between different bacterial genera. Here, we developed a method to quantify the number of HAE and HME RND transporter proteins encoded in a genomic sequence based upon conserved residues in characterized RND transporter proteins. To do this, the sequences of 24 known RND pump genes from 16 species were aligned to determine the conserved residues which could be used to search for known and unknown RND pump genes in genome sequences of Gram-negative bacteria. Due to the degree of difference in sequences between HAE and HME pumps, two separate alignments were created. From each alignment, residues that were the same in 80% of sequences or more were used to create a conserved residue file, with which BLASTp could search genomes to determine the number of each type of RND pump (Supplementary S3, texts S1–2). To validate this method, the number of RND transporters in well-characterized type strains of Gram-negative bacteria were determined (Table 1).

For *A. baumannii*, *C. jejuni*, *E. coli*, *H. influenzae*, *N. gonorrhoeae*, *P. aeruginosa*, *K. pneumoniae* and *Shigella flexneri* the number of inner membrane RND efflux pumps detected using our method matched that in the literature for the species tested, validating this approach. For example, *N. gonorrhoeae* is well known for encoding only one RND protein [66] and this was also true when FA1090 (NC_002946.2) was tested using our method. For *E. coli* K12, all seven known RND proteins were detected, including the HME protein CusA. CusA was identified in both the HAE and HMD RND protein searches, but is only included once in Table 1. Interestingly, we were also able to find an additional RND protein in *Salmonella enterica* serovar Typhimurium, annotated as OqxB by Prokka [37].

In *A. baumannii* AYE, however, the BLASTp searches only identified five out of six known RND pump proteins. Both HAE and HMD searches failed to highlight ArpB, an RND-like protein that is involved in opaque to translucent colony formation switching [27]. ArpB was added to both the HAE and HME alignments, but due to differences in the sequences of the other RND proteins compared to it, the number of conserved residues reduced dramatically across the aligned proteins and rendered the method unable to then detect any RND pump proteins successfully via BLASTp. Phylogenetic trees based upon the alignments with ArpB are shown in Supplementary S1, Figs S3 and S4, and show that ArpB clusters separately from the other proteins. Interestingly, when using BLASTp to estimate the number of HAE RND proteins across 100 sequences of *A. baumannii* (including *A. baumannii* ACICU), in 95% of the sequences all five proteins were detected (Supplementary S2, Table S4). This suggests that ArpB can be identified by the search and that the sequence of ArpB in *A. baumannii* AYE differs from that of other *A. baumannii* sequences. When directly comparing the amino acid sequence of ArpB from AYE and ArpB from ACICU, they are only 24.5% identical with a coverage of 94%.

Table 1. Number of inner membrane RND proteins within the genomes of Gram-negative bacteria, as determined by BLASTp of the conserved RND residues using HAE and HME databases (S3 text 1–2)

Species	RefSeq accession	No. of predicted HAE proteins	No. of predicted HME proteins	Total no. of proposed RND proteins in the literature (reference)
<i>Acinetobacter baumannii</i> ACICU	NC_010611.1	5	1	6 [81]
<i>Acinetobacter baumannii</i> AYE	NC_010410.1	4*	1	6 [81]
<i>Campylobacter jejuni</i> NCTC 11168	GCF_900475265.1	2	0	2 [11]
<i>Escherichia coli</i> K12	NC_000913.3	6	1	7 [91]
<i>Haemophilus influenzae</i> NCTC 8143	GCF_001457655.1	1	0	1 [92]
<i>Klebsiella pneumoniae</i> ATCC 43816	NZ_CP064352.1	8	1	9 [11, 93, 94]
<i>Neisseria gonorrhoeae</i> FA1090	NC_002946.2	1	0	1 [66]
<i>Pseudomonas aeruginosa</i> PAO1	GCF_000006765.1	10	1	11 [11]
<i>Shigella flexneri</i> 5a M90T	NZ_CP037923.1	5	1	6 [95]
<i>Salmonella enterica</i> serovar Typhimurium SL1344	NC_016810.1	6	0	5 [11]

**A. baumannii* AYE results were missing ArpB due to sequence dissimilarity with the RND proteins used in our alignments. This is discussed further below.

Salmonella enterica Typhimurium is shown separately at the bottom because an additional RND efflux protein, to those described in the literature, was found.

Of the 100 *A. baumannii* sequences analysed, 95% encoded five HAE RND proteins, 3% had four, and 2% had six or seven. In the three sequences that had only four RND proteins, they were missing AdeB and a subsequent targeted BLASTn search for *adeB* provided no results. The additional RND protein in the other two sequences (GCA_000302135.1 and GCA_000301875.1) is currently not characterized and when looking more closely at the seventh protein identified in GCA_000301875.1, it seems to be a truncated RND protein with amino acid sequence similarity (99%) to AdeB and found next to ArpB.

In the 100 *A. baumannii* sequences, the number of HME pumps also differed within the species. In total, 67% of sequences had only one heavy metal pump protein – CzcA (Supplementary S2, table S5). Although another inner membrane protein (CzcD) exists in the Czc system, its sequence is much shorter than the HME proteins in the alignment, so it is not found using the BLASTp search. The remaining sequences had an additional one to three proteins encoded in their genomes. In total, 27% had a total of two HME proteins, CzcA and a protein annotated as CusA. Furthermore, 5% had three HME proteins where the third protein was also labelled as CzcA, but was not found with CzcD, so it is likely to be annotated incorrectly and could represent a third distinct heavy metal efflux system in *A. baumannii*. Finally, one sequence (GCA_000307895.1) had four HME proteins and three of them were annotated as CzcA (genomic positions 4668–7796, 6237–9395 and 12251–15379 bp) and one as CusA. Of the three CzcA, two were found in an operon with other Czc proteins and the other one is a protein with an amino acid sequence similar (100% identity) to CzcA/CusA family proteins but not located near other Czc protein-encoding genes.

Table 1 shows that not only does the method to identify RND pump proteins work across a broad range of Gram-negative species, it has also highlighted uncharacterized inner membrane RND proteins within genomes. The method was further applied to determine the number of RND pump proteins in every species of the *Acinetobacter* genus (Fig. 1, column 1).

The number of RND proteins differs across the genus *Acinetobacter*

The number of inner membrane RND pump proteins in species of *Acinetobacter* ranged from two to nine (Fig. 1, column 1), and this correlated with whether that species is known to cause human infection. Via a point biserial Pearson's correlation, the number of RND proteins and ability to cause infection was positively correlated ($r_{pb}=0.376$, $n=65$, $P=0.002$), which was statistically significant. Therefore, infection causing species generally encoded more RND transporter genes than those that have not been reported to cause infection. Whilst there are likely to be more *Acinetobacter* species that have the capacity to cause human infection, the heatmap just documents those published to date.

Previous work has shown that not all species have the same number of total RND components; for example, in *A. baumannii* around 20% of all isolates are missing the OMF AdeC and up to 25–30% have been shown to be missing the RND protein AdeB [24, 33, 67]. This is also evident in our data; whilst the number of RND proteins differs across the genus *Acinetobacter*,

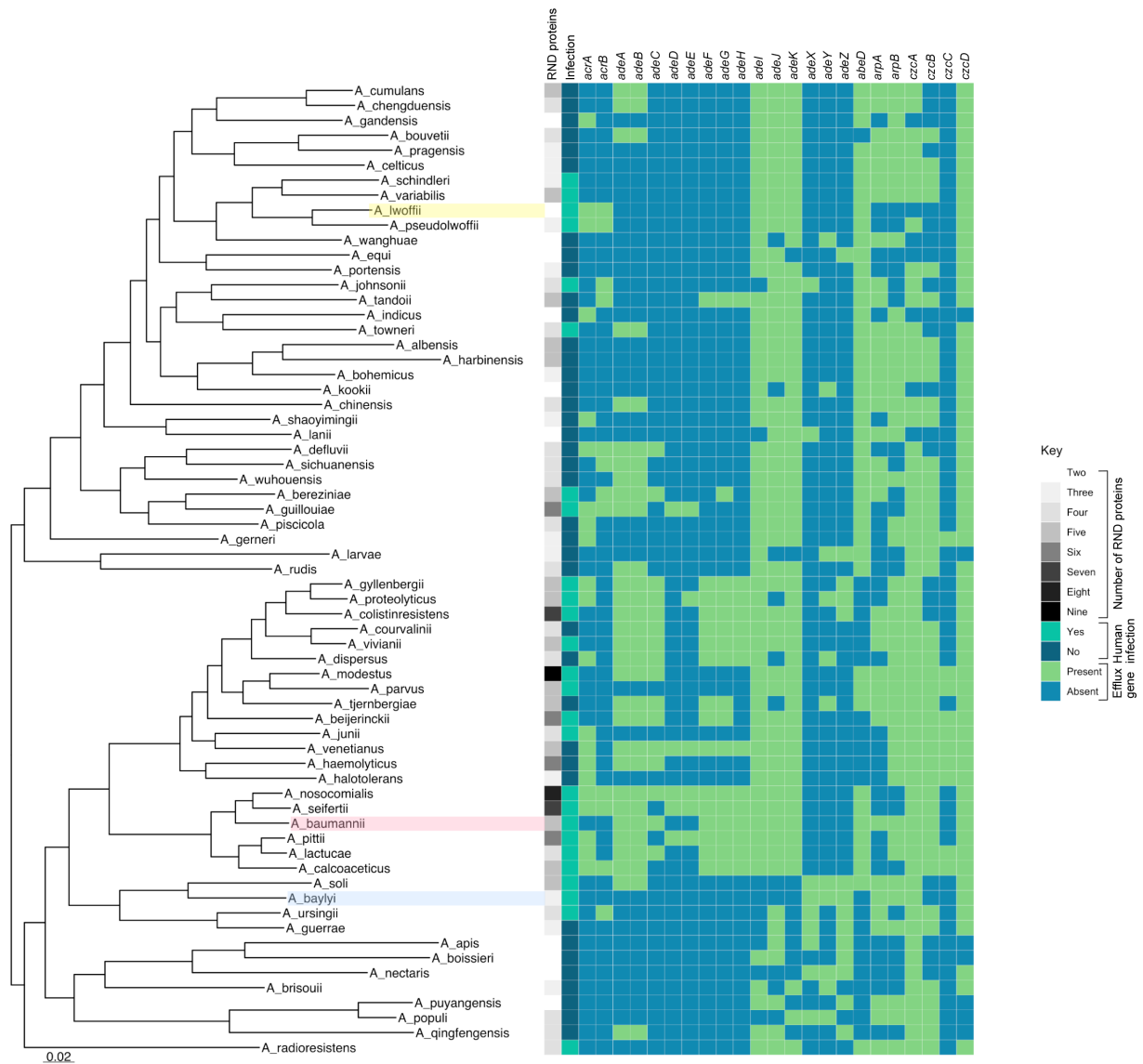


Fig. 1. The presence of RND pumps across the genus *Acinetobacter*. Heatmap of the genus *Acinetobacter* with characterized RND genes presence/absence and the number of RND proteins. A phylogenetic tree of the species that make up *Acinetobacter* is shown on the left-hand side, created using a core gene alignment. For column 1, the number of RNDs, the mean average of the total number of (both HME and HAE) RND efflux proteins for each species was determined, to one significant figure, where the greater the number of proteins, the darker grey the colour. For column 2, if a species has been shown in the literature to cause infection it is turquoise. Subsequent columns 3–25 are highlighted green if the efflux gene was found in the reference sequences using ABRicate. *A. lwoffii* is highlighted in yellow, *A. baumannii* pink and *A. baylyi* blue. Scale bar represents the branch length for a genetic change of 0.02.

the number of RND proteins also differs between members of the same species. For example, in *A. colistiniresistens* sequences there were between three and five HAE RND proteins and between one and four HME RND proteins. The mean average of the total RND proteins, seven, highlighted in the four *A. colistiniresistens* sequences tested is shown in Fig. 1. Furthermore, this variation is seen in other species such as *A. bereziniae*, where three or four HAE and one to three HME proteins were highlighted as well as in *A. haemolyticus*, *A. pittii*, *A. proteolyticus*, *A. tandoii* and above in the 100 *A. baumannii* sequences.

Presence of RND efflux pumps across the genus *Acinetobacter*

To gain a broader picture of what RND system genes, including PAP genes and OMF genes, are present in the genus *Acinetobacter*, genomes from all validated *Acinetobacter* species were searched for the presence of these genes using a custom database of *Acinetobacter* RND genes in ABRicate (Supplementary S3, text S4). Fig. 1 shows a heatmap in which the presence (green) and absence (blue) of RND genes is mapped onto a phylogenetic tree of the genus. The average number of RND proteins, as

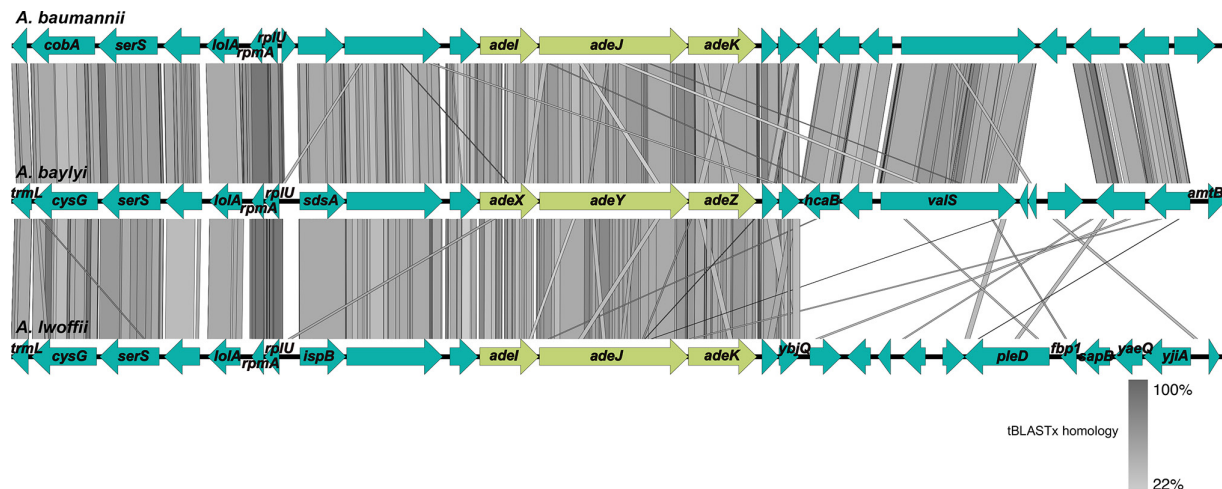


Fig. 2. The genomic context of *adeIJK* and *adeXYZ* is identical. The figure was created in Easyfig (v.2.2.5) using *A. baumannii* AYE (NC_010410.1), *A. baylyi* ADP1 (NC_005966.1) and *A. lwoffii* 5867 (GCA_900444925.1) sequences plus and minus 10 kb from the *ade* operons, annotated using Prokka [37]. The grey scale shows tBLASTx homology and arrows refer to coding regions within the genome. Immediately around *adeIJK/XYZ* is conserved but differs further downstream of the OMF. *A. baumannii* and *A. baylyi* are more similar downstream of the OMF, compared to *A. lwoffii*. The two genes immediately after each OMF are genes which encode YbjQ family proteins and this is conserved in all three species (*A. baumannii*: HK016_14475, HK016_14480, *A. baylyi*: KJPEBFEL_02742, KJPEBFEL_02743, *A. lwoffii*: NCTC5867_02643, *ybjQ*). The gene immediately upstream of *adel/X* is a gene encoding a PAP2 phosphatase family protein (*A. baumannii*: HK016_14455, *A. baylyi*: KJPEBFEL_02738, *A. lwoffii*: NCTC5867_02647).

determined by the novel RND residue BLASTp search, is also plotted in greyscale (column 1). The average number of RND proteins sometimes over- or underestimates the number compared to the RND genes found by ABRicate, because ABRicate searched only one reference sequence and the number of RND proteins is the average of up to four sequences searched by BLASTp. When directly comparing the same sequence using BLASTp to search for proteins with conserved RND residues and ABRicate to highlight all characterized RND genes, BLASTp finds the same or more efflux pump proteins compared to ABRicate in 38 species. In the remaining 27 species, BLASTp found 75% of the RND proteins highlighted by ABRicate. Therefore, a combination approach of both methods provides the best resolution when looking for RND genes and proteins. In total BLASTp found 274 proteins with conserved RND residues and ABRicate found 272 characterized RND transporter genes.

Parts of the metal ion efflux system, *Czc*, are also common across the genus where *czcD* and *czcA*, coding for the inner membrane proteins, are found in almost all species. In contrast, other RND systems, such as *adeABC* and *adeFGH*, are commonly found in a clade consisting of *A. baumannii* and closely related species, which have a higher propensity to cause human infection.

Notably, almost all *Acinetobacter* species encode *adeIJK* and it is striking that those that do not, encode the *adeXYZ* operon instead. This is true in all but three species, *A. colistiniresistens*, *A. gyllenbergii* and *A. proteolyticus*, which encode genes that are similar to both *adeK* and *adeZ* according to the ABRicate search. Indeed, when looking more closely at these, it seems that they have a full *adeIJK* operon, but also an additional RND operon with an OMF that is 69–71% identical to *adeK*, found with a PAP and RND protein. In addition to the three species that encoded parts of *adeIJK* and *adeXYZ*, *A. cumulans* encoded two complete copies of the *adeIJK* operon.

***A. baumannii* *adeIJK* and *A. baylyi* *adeXYZ* are homologous efflux systems**

Originally, *adeXYZ* was described in *A. baylyi* and stated to have high sequence similarity to *adeIJK* from *A. baumannii* [24, 68]. The fact that the absence of *adeIJK* in Fig. 1 seems to match almost perfectly to the presence of *adeXYZ* suggested that these pumps may be divergent examples of the same pump, rather than distinct systems. Therefore, the sequence, genomic location, function and structure of *adeIJK* from *A. baumannii* AYE, and *adeXYZ* from *A. baylyi* ADP1 were compared. In addition, another *adeIJK* from a more phylogenetically distant *Acinetobacter* (*A. lwoffii* 5867) was included for context.

In *A. baumannii* AYE, *A. lwoffii* 5867 and *A. baylyi* ADP1, the *adeIJK* and *adeXYZ* operons are found in the same genomic location, with conserved regions up- and immediately downstream of the operon (Fig. 2). The genes flanking the *adeIJK/XYZ* operons encode PAP2 phosphatase family proteins and YbjQ family proteins. Despite the high level of conservation around the operons, downstream from the OMF the sequences differ dramatically. Neighbouring genes that could be annotated by Prokka [37] are also included in Fig. 2, but there are discrepancies where homologous genes are annotated differently in different species.

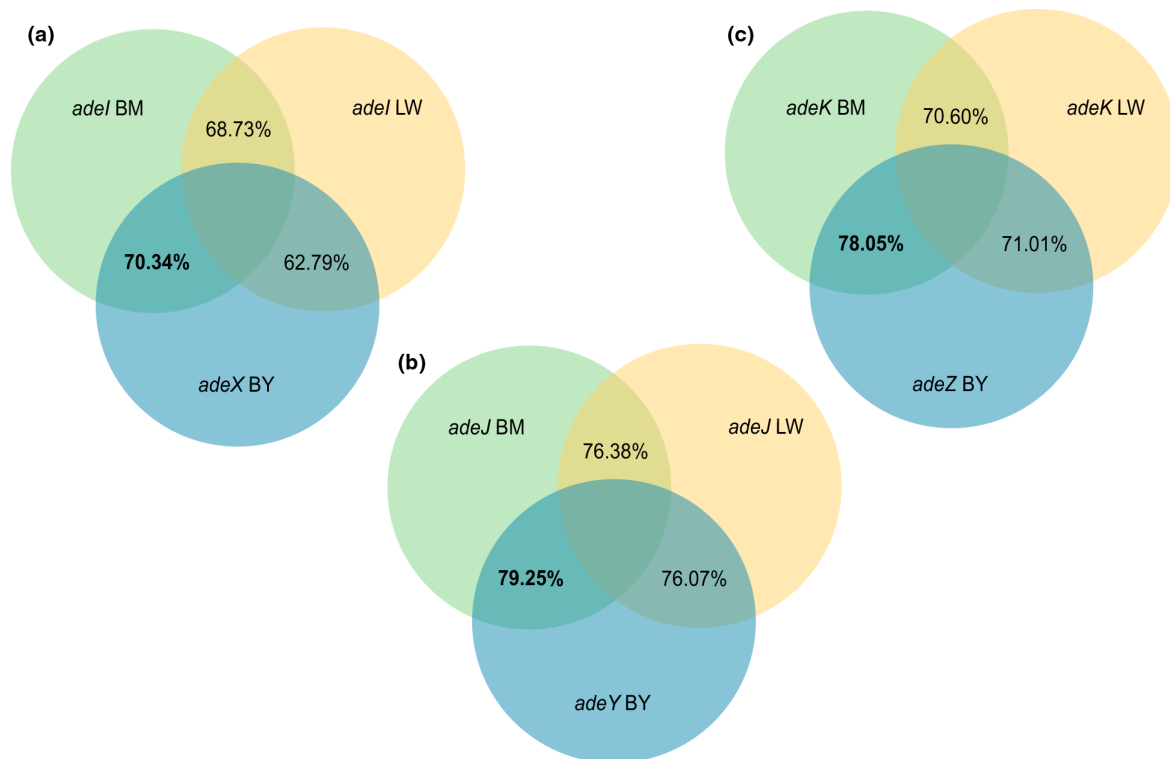


Fig. 3. Venn diagrams of percentage identity between *Acinetobacter* RND genes. Percentage identity was determined by a MAFFT (v.7) alignment of the PAP, RND and OMF genes, which was analysed by Sequence Manipulation Suite [96]. BM, *A. baumannii* (green); LW, *A. lwoffii* (yellow); BY, *A. baylyi* (blue). (a) PAP, (b) RND, (c) OMF. In bold are the most similar pair for PAP, RND and OMF based upon percentage nucleotide identity. PAP genes (ABAYE0748, DY357_RS13160, ACIAD_RS13290), RND genes (ABAYE0747, DY357_RS13155, ACIAD_RS13295) and OMF genes (ABAYE0746, DY357_RS13145, ACIAD_RS13300).

The periplasmic adaptor protein genes, *adeI* and *adeX*, in *A. baumannii*, *A. lwoffii* and *A. baylyi* are 62–70% similar. The sequence of *adeI* from *A. baumannii* is more similar to *adeX* from *A. baylyi* than *adeI* from *A. lwoffii*. The same pattern can be seen for the RND (*adeJ/Y*) and OMF (*adeK/Z*) genes, where the nucleotide sequences from *A. baumannii* for each component of the tripartite pump are more like the sequences from *A. baylyi* than *A. lwoffii*, despite them sharing the nomenclature with *A. lwoffii* (Fig. 3).

Given that *adeIJK/XYZ* is found in all *Acinetobacter*, but *adeABC* and *adeFGH* are found only in a subset of species, the recombination levels and polymorphisms in and around all three *ade* operons were analysed. To determine if there were any recombination hotspots and polymorphisms around *adeIJK*, Gubbins was used to infer recombination levels across the whole genomes of 100 *A. baumannii* sequences. Fig. 4 shows the recombination predictions for *adeABC* (e and f), *adeFGH* (c and d) and *adeIJK* (a and b) across the sequences. Of the three systems, there is no signature of recombination seen around the *adeIJK* genes across these sequences, indicating this is an ancestral operon common across all genomes studied here. High levels of recombination are seen around *adeABC* and because it is found in *A. baumannii* and other infection-causing species (Fig. 1) but not all *Acinetobacter*, it is likely that this operon is in a recombination hotspot where genes are acquired by horizontal gene transfer. Polymorphisms are also shown in Fig. 4 (red and blue blocks), where more are seen around AdeABC. Further to this, the level of recombination and polymorphisms is also low around *adeFGH*.

The phenotypic impact of *adeIJK* and *adeXYZ* expression is the same

To determine whether the substrate profile of AdeIJK and AdeXYZ are the same, *adeIJK* from *A. baumannii* AYE and *adeXYZ* from *A. baylyi* ADP1 were cloned and expressed in *A. baumannii* ATCC 17978 UN Δ *adeAB* Δ *adeFGH* Δ *adeIJK* and susceptibility to known substrates of different Ade systems was measured. The effect of expression of AdeIJK and AdeXYZ in ATCC 17978 Δ *adeAB* Δ *adeFGH* Δ *adeIJK* was identical, with both conferring decreased susceptibility to chloramphenicol, ciprofloxacin, clindamycin, tetracycline and rifampicin.

Initially, these plasmids were expressed in ATCC 17978 lacking only *adeIJK* (Δ *adeIJK*), which increased the ethidium bromide (EtBr) MIC from 1 to 64 μ g/mL¹ (data not shown). However, in the triple pump deletion background Δ *adeAB* Δ *adeFGH* Δ *adeIJK*, expression

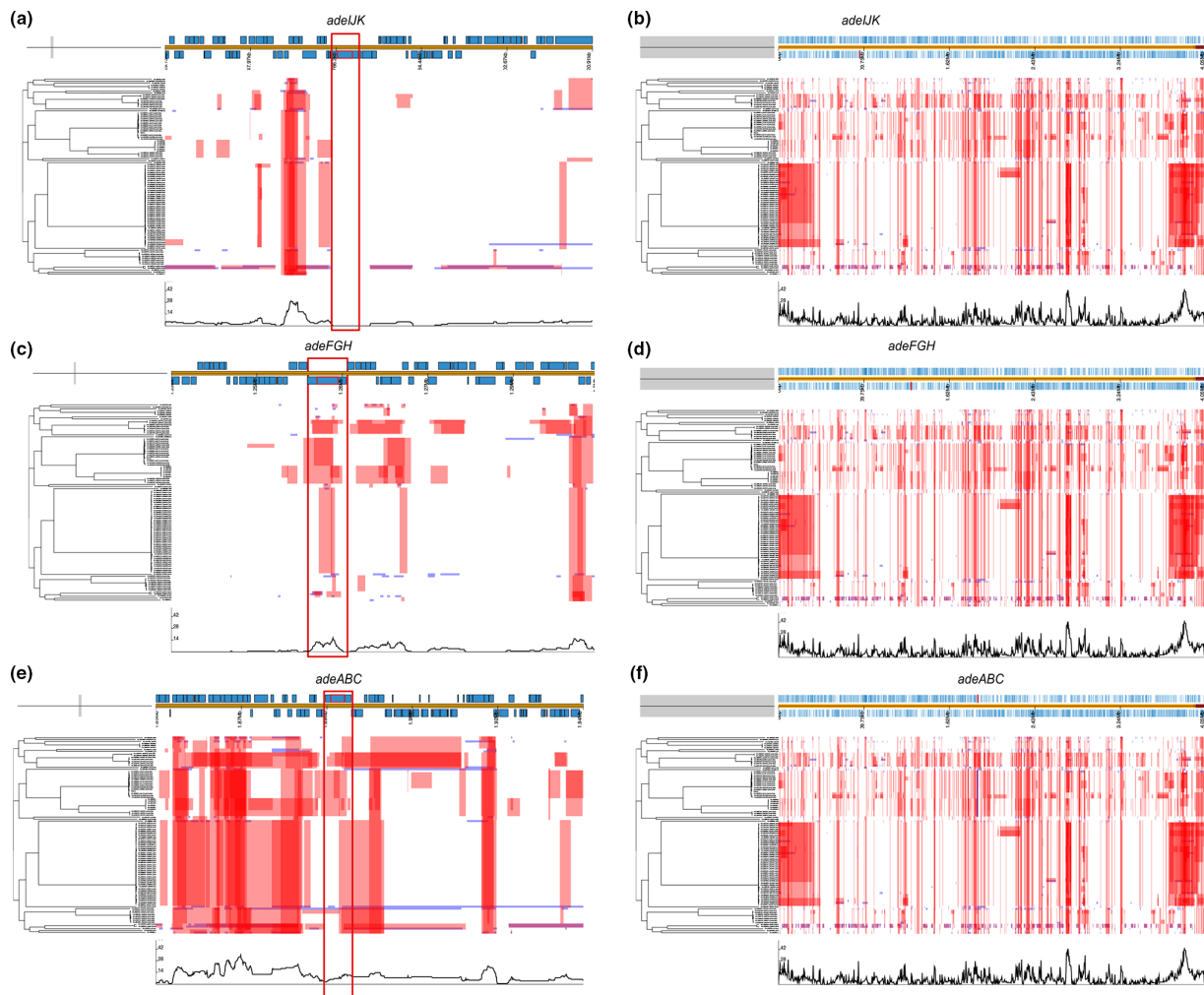


Fig. 4. AdeIJK has fewer SNPs within it and lower levels of recombination surrounding it than AdeABC or AdeFGH. In total, 100 *A. baumannii* genomes were aligned against reference *A. baumannii* AYE (NC_010410.1) and the presence of polymorphisms and recombination was determined using Gubbins. (a,c,e) Magnified parts of the genome at each *ade* operon, showing the levels of SNPs (red and blue squares; red are ancestral SNPs) and recombination levels (the black line on the bottom; the higher the peak the more recombination). The right-hand panels (b, d and f) show the entire genome and the position of each different *ade* operon, which is highlighted in red beneath the label. All panels have an associated mid-point rooted phylogenetic tree created by Snippy to show the relatedness of the *A. baumannii* sequences. AdeIJK (a) has fewer SNPs and recombination than AdeABC (e) and AdeFGH (c), indicating it is highly conserved.

of neither AdeIJK nor AdeXYZ altered susceptibility to EtBr (Table 2), suggesting AdeIJK does not export EtBr as shown previously [23]. The basis for this difference in relation to strain background is not fully understood but has been reported previously [23].

AdeJ from *A. baumannii* and AdeY from *A. baylyi* are structurally similar

Since AdeIJK from *A. baumannii* and AdeXYZ from *A. baylyi* are genetically and functionally similar, we next examined whether their respective RND transporters also shared similar structural features using comparative analysis of the experimentally available structures and making homology models of the missing ones. Again, *A. lwoffii* AdeJ was included for context.

High-fidelity homology modelling of AdeJ from *A. lwoffii* (76.38% identity) and AdeY from *A. baylyi* (79.25% identity) was enabled by recent determination of the experimental structures of AdeJ from *A. baumannii* (*AbAdeJ*) in both apo- and eravacycline-bound forms (7M4Q.pdb and 7M4P.pdb, respectively [54]). The amino acid sequences of AdeJ from *A. baumannii* (*AbAdeJ*), *A. lwoffii* (*AlAdeJ*) and *A. baylyi* AdeY align without any gaps, allowing for one-to-one positional correspondence between them (Fig. 5), with the sole exception of a single residue insertion after position 602 (*AbAdeJ* numbering) in both *A. lwoffii* AdeJ and AdeY, which maps to the protein surface (PC1 sub-domain), and thus should not directly affect drug binding. There is also a high level of conservation with other members of the RND-transporter family, including AdeB

Table 2. Broth microdilution MIC results ($\mu\text{g/mL}$) for AdeJJK and AdeXYZ when expressed in *A. baumannii* ATCC 17978 $\Delta\text{adeAB } \Delta\text{adeFGH } \Delta\text{adeIJK}$

Strain	Chloramphenicol	Ciprofloxacin	Clindamycin	Tetracycline	Ethidium bromide	Rifampicin
RND systems known to export	AdeABC, AdeFGH, AdeIJK	AdeABC, AdeFGH, AdeIJK	AdeFGH, AdeIJK	AdeABC, AdeIJK	AdeABC	AdeIJK
Presumed efflux routes	DBP	DBP	DBP	DBP/PBP	DBP	PBP
WT	64	16	64	2	>256	4
KO	8	8	4	0.25	1	2
<i>padeIJK</i>	512	128	16	8	1	8
<i>padeXYZ</i>	512	128	32	8	1	8

WT = *A. baumannii* ATCC 17978; KO = *A. baumannii* ATCC 17978 $\Delta\text{adeAB } \Delta\text{adeFGH } \Delta\text{adeIJK}$ + empty pVRL2 vector; *padeIJK* = *A. baumannii* ATCC 17978 $\Delta\text{adeAB } \Delta\text{adeFGH } \Delta\text{adeIJK}$ + Abaum *adeIJK* pVRL2; *padeXYZ* = *A. baumannii* ATCC 17978 $\Delta\text{adeAB } \Delta\text{adeFGH } \Delta\text{adeIJK}$ + Abayl *adeXYZ* pVRL2.

[57, 69], AcrB [18, 56] and MtrD [58]. Indeed, the very close geometry of these transporters, with the superposition of the AdeJ structure and the ligand-occupied T-conformers AcrB (7M4P:B and 4D \times 5:B respectively) yielded a strikingly low root mean square deviation of 1.17 Å, allowing for direct comparison and interpretation of their binding pockets (supplementary S4, Fig. S5). As our current knowledge of substrate recognition within RND pumps derives primarily from AcrB, this close relationship allows for an unambiguous assignment of the binding determinants between the pumps. Accordingly, analysis of the residues lining the PBP and the DBP, which are implicated in the processing of the high-molecular-weight (including macrolides and rifampins) and lower-molecular-weight/planar compounds (e.g. tetracyclines, fluoroquinolones and beta-lactams) respectively [18, 56, 57, 70], identified high levels of positional conservation of the residues previously described as forming the recognition determinants of these binding pockets [18, 19, 56] (annotated in Fig. 5) between AdeJ and AdeY, fitting with the antimicrobial susceptibility data in Table 2 and suggesting an identical substrate profile. A detailed description of the residue conservation within the respective binding pockets and comparison to other RND-transporters is provided in Supplementary S4 text 4 and Table S6.

The PBP is generally conserved amongst RND transporters, except for the residue range 660–688 (*AbAdeJ* numbering), which forms the bottom section of the PBP and covers the so-called F-loop (Fig. 5). Strikingly, while this region displays near-complete conservation between AdeJ and AdeY (the only minor exception being T679, which in *A. lwoffii* is represented by a conservative substitution to serine), it shows major deviation from both the *AbAdeB* [54, 69, 71] and *E. coli* and *Salmonella* AcrB [72, 73]. The AdeJ/Y PBP also features a diagnostic V573, which is strictly conserved amongst them, but not present in other RND transporters, providing a clear differentiation of the AdeJ and AdeY pumps. Another prominently conserved residue within the AdeJ/Y subfamily is found in the front of the PBP, corresponding to R718 in *AbAdeJ* (Supplementary S4 Fig. S6, panel B). It is notable that R718 is conserved in AcrB/MtrD/MexB transporters, but not in the paralogous AdeB, which suggests a closer relationship of the AdeJ/Y to the former. The AdeJ/Y proteins clearly cluster separately from other Gram-negative RND proteins, including AdeB (Supplementary S4, Fig. S7). Taken together, the above conservation analysis suggests a common mode of substrate recognition in the PBP of AdeJ and AdeY, again highlighting their close relationship to each other.

The PBP and DBP are separated by the flexible G-loop (covering the residue range 613–624 in *AbAdeJ*), which contains a conserved phenylalanine (F618), which is involved in drug binding in the DBP of both the newly determined AdeJ fluorocycline-bound structures [54, 74], and in AdeB [69]. Amongst AdeJ/Y, the whole of the G-loop is strictly conserved, again suggesting similar binding properties in the upper part of the PBP and the front part of the DBP.

Moving to the DBP, the *AbAdeJ* residues F136, F178, Y327, V613, F618 and F629 are universally conserved across AdeJ/Y, AcrB/MtrD and AdeB-transporters. Again, amongst the AdeJ/Y family members, there are very few substitutions (Fig. 5), but it is striking that three out of four that are present (A46, Q91 and T128), are clustered together at the back of the pocket (Supplementary S4, figure S6, panel C), forming a plausible interaction site, suggested by the apparent covariation of the residues occupying positions 46 and 128. While in *A. baumannii* this pair is represented by A46/T128, in *A. lwoffii* and *A. baylyi* it is instead an S46 in combination with either R128 or K128 respectively. The last DBP residue to show variation within the AdeJ/Y subfamily is Y327 (F327 in *A. lwoffii*), and is found at the bottom of the pocket, on the opposite side across from the A46/T128 pair (Supplementary S4, Fig. S6, panel C). Intriguingly, it is in direct contact with M575, itself a variable residue, forming the front of the PBP, and also interacting with the variable PBP residue T679 mentioned above.

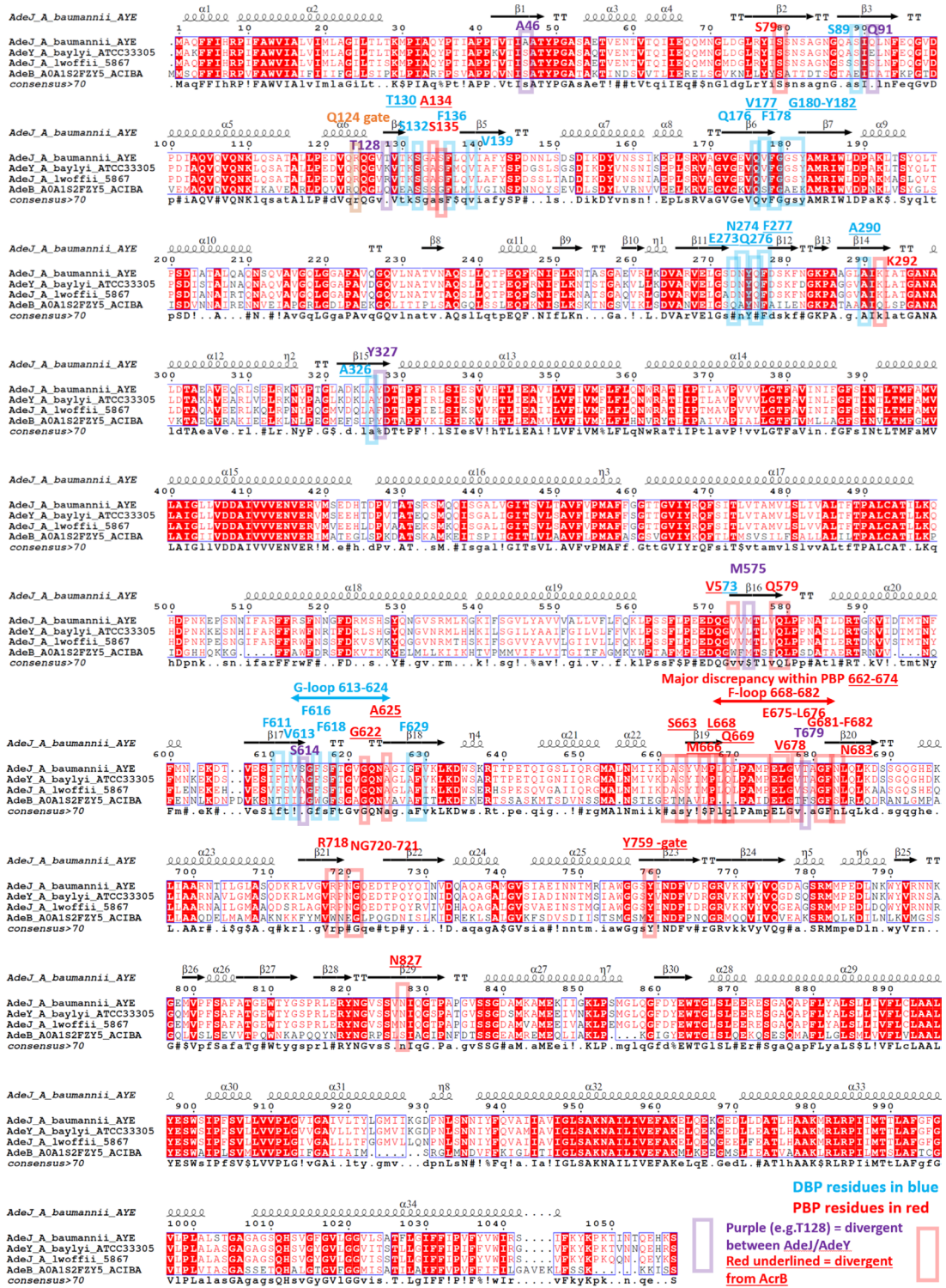


Fig. 5. Sequence alignment of AdeJ/Y and AbAdeB, highlighting the key binding determinants in the distal binding pocket (DBP) (blue boxes/font) and proximal binding pocket (PBP) (red boxes/font). The alignment shows the close relationship between AdeJ and AdeY, and positional equivalence between the members of AdeJ/Y clade. Residues within the drug-binding pockets that are divergent within the AdeJ/Y clade are highlighted in purple. Secondary structural elements were derived from the experimental AbAdeB structure 7M4P.pdb. The consensus sequence is displayed in the bottom row. Accession codes for the respective sequences used are as follows: AdeJ *A. baumannii* Uniprot ID: Q2FD94; AdeB *A. baumannii* Uniprot ID Q2FD70; AdeJ *A. lwofii* WP_253174392.1; AdeY *A. baylyi* WP_011182646.1. Figure prepared with ESript 3.0 [59].

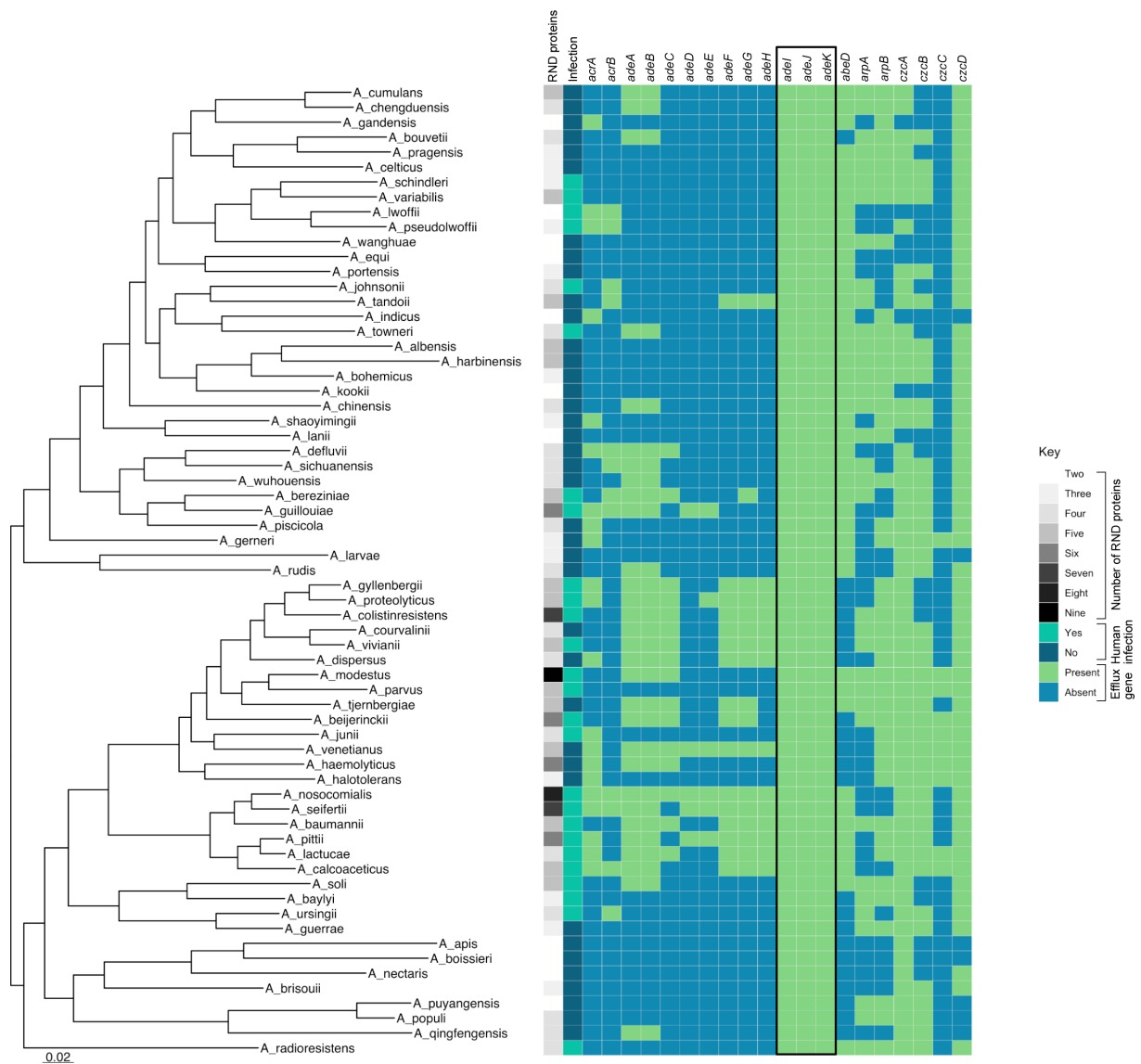


Fig. 6. AdeJK is the ancestral efflux pump in the genus *Acinetobacter*. Heatmap of the genus *Acinetobacter* with characterized RND genes presence/absence and the number of RND proteins. For column 1, the number of RNDs, the mean average of the total number of (both HME and HAE) RND efflux proteins for each species was determined, to one significant figure, where the greater the number of proteins, the darker grey the colour. For column 2, if a species has been shown in the literature to cause infection it is turquoise. Subsequent columns 3–22 are highlighted in green if the efflux gene was found in the reference sequences using ABRicate. The *adeJK* and *adeXYZ* columns were amalgamated (black box) in this heatmap because they are the homologues, for clarity. Scale bar represents the branch length for a genetic change of 0.02.

In summary, structural analysis of the AdeJ and AdeY transporters reveals that they share a number of distinguishing features that are common across them, but distinctive enough to set them apart as a separate group within the wider RND family. These include major changes in the PBP, including the entire F-loop region, which is highly divergent from other RND transporters. At the same time, the overall high conservation of the DBP, combined with the presence of the R718 residue, helps to explain their identical substrate profile (Table 2), while suggesting a closer functional alignment to AcrB/MtrD/MexB transporters than to the paralogous AdeB.

Thus, based on the genetic, structural and phenotypic similarities between *adeJK* and *adeXYZ*, we propose that *adeXYZ* should be named *adeJK* and we have hence amalgamated the two systems in the heatmap in Fig. 6, which now shows the presence of *adeJK* in every described *Acinetobacter* species.

DISCUSSION

The number of RND efflux genes per genome differs at both the genus and species levels. Novel RND pumps are being characterized continually and it is likely there are many yet to be discovered. Due to the broad roles that RND pumps have within cells, fully understanding the complement of systems within a given species is important, especially when trying to understand MDR phenotypes in pathogens. We have presented a simple way to screen for HAE and HME RND proteins encoded in bacterial genomes based upon conserved residues, which highlighted both known RND pump proteins and uncharacterized ones in a variety of Gram-negative species. There are some limitations to the method as very divergent RND pump systems, such as ArpB, may not be detected. A combination approach of searching for known efflux genes and using the conserved residue RND protein search provides the best insight into the complement of RND systems in a given species.

The number of RND transporter proteins differs between species of *Acinetobacter* and also within species, but this is somewhat limited by the number of sequences tested per species. In *Acinetobacter*, there were between two and nine RND proteins in any given genome sequence, where *A. nosocomialis* and *A. modestus* had the most RND genes. Species that cause human infection encoded more RND proteins. Previous work has shown that by over-expressing the RND genes *adeABC*, *A. baumannii* is more virulent in the lungs of a mouse [75], and the role of RND pumps in infections has also been noted in other Gram-negative bacteria including *N. gonorrhoeae* (MtrCDE), *Salmonella enterica* (AcrAB-TolC), *Pseudomonas aeruginosa* (MexAB-OprM), *Campylobacter jejuni* (CmeABC) and *Vibrio cholerae* (VexB/D/K) [76–80]. Subsequent work is needed to fully elucidate if there is a link between the number of RND proteins and a species' ability to cause infection in humans across the genus *Acinetobacter*. In this study, 64 *Acinetobacter* species were characterized at the time the analyses were done, but since then further *Acinetobacter* species have been described. Additionally, when looking at RND pump proteins within *A. baumannii*, almost all sequences had the five characterized RND proteins but there was some variation, with some sequences lacking AdeB, which has been seen previously in *A. baumannii* isolates [24, 33].

The RND system *adeIJK* was found to be present across *Acinetobacter*, and isolates without it encoded *adeXYZ*, which led us to investigate if these systems are actually the same. The MIC data show that both AdeIJK and AdeXYZ can export the same compounds, including tetracycline, chloramphenicol and clindamycin, which have previously been identified as substrates for AdeIJK [81]. Exact values were not directly comparable to previous studies as different expression systems were used. The pVRL vectors are high copy number plasmids explaining why some MICs increased above that of the wild-type strain. Very high levels of expression of AdeIJK have previously been shown to be toxic in both *A. baumannii* and *E. coli* [23] and correspondingly we were unable to successfully express AdeIJK in *E. coli* despite testing a range of vectors.

Homology modelling supported the data suggesting identical substrate profiles to the structure of AdeJ and AdeY, and in particular their binding pockets were highly similar.

Our structural analysis also confirmed the common structural features of AdeJ/Y, which justifies isolating them as a separate subfamily of RND transporters. Indeed, while the overall architecture, and correspondingly the structure of the drug-binding pockets, is conserved across AdeJ/Y, they show unique features that clearly distinguish them even from closely related RND relatives. In the interests of space, a detailed discussion of residue conservation is provided in Supplementary S4, text S4, but a few noteworthy elements are highlighted below.

The differentiating features of AdeJ/Y include the organization of the principal drug-binding pockets, with in particular the base of the PBP displaying clear differences from other members of the RND family, including the so-called F-loop (Fig. 5; supplementary S4, Fig. 6b). Indeed, the F-loop is different not only between AdeJ/Y and AdeB, but also between AdeJ/Y and AcrB/MtrD. It seems likely that this discrepancy may be contributing to the differential substrate efflux efficiencies between AdeB and AdeJ/Y reported previously [82].

The PBP also features a diagnostic V573, which is only present within the AdeJ/Y subfamily, providing differentiation from other transporters. In addition, AdeJ/Y also display some hybrid features, linking them to the canonical MDR transporters. These include the presence of an arginine (R718 in AdeJ/Y), which forms the front part of the PBP (substrate channel 2 exit) [70, 83], and which is conserved across AcrB/MtrD/MexB (R717 in AcrB) [18, 58, 84], where it has been implicated in binding of the macrolides and rifamycins [57, 58, 85, 86]. This critical residue is not conserved in AdeB however, suggesting that AdeJ/Y probably process their substrates more similarly to AcrB/MtrD than to AdeB. This is further supported by our analysis of the DBP, where only four residues have been shown to have limited variability within the analysed AdeJ/Y structures. As mentioned above, three out of four variable residues (A46, Q91 and T128) are clustered together at the back of the pocket and display positional covariation (supplementary S4, Fig. S6, panel C), suggesting functional interaction between them and formation of a plausible interaction site, which could be responsible for distinctive DBP ligand coordination and warrant further investigation beyond the remit of the current study. The additional conservation of the residues within the DBP, including the critical ligand-binding residues such as AcrB F610 (corresponding to AbAdeJ F611), across AcrB/MtrD/MexB, but not AdeB again suggests a closer relationship of AdeJ/Y to the former.

The clear distinction of AdeJ/Y from AdeB, and the closeness of AdeJ/Y instead to AcrB/MtrD/MexB, suggest that AdeJ/Y represent the basal efflux pumps within the genus, while AdeB paralogues may have been acquired within the genus *Acinetobacter*.

Together, the genetic, structural and phenotypic data presented show that AdeIJK and AdeXYZ are in fact divergent homologues of the same system and we propose that *adeXYZ* should be named *adeIJK*. As shown in Fig. 6, this highlights the presence of *adeIJK* in every *Acinetobacter* species studied to date, indicating it is under high selection pressure, providing an important function. This further agrees with our recombination analysis, which showed the lowest levels of recombination around *adeIJK*, when compared to *adeABC/adeFGH*. A recent study also looked into recombination within antibiotic resistance genes and found that *adeJ* and *adeK*, but not *adeI*, were affected by recombination [87]. This is in contrast to what we report, and whilst the present paper was in review another paper has been published showing that *adeIJK* genes are highly conserved across *Acinetobacter*, supporting our results with respect to recombination and levels of polymorphisms across *adeIJK* [88]. The reason for the presence of *adeIJK* across all species in the genus might be due to the wide roles that *adeIJK* carries out in *Acinetobacter*, for example its ability to protect against antibacterial host-associated fatty acids and modulate the bacterial cell membrane [82]. Furthermore, *adeIJK* plays a role in virulence, biofilm formation and surface motility and can export a broad range of compounds, including clinically relevant antibiotics, providing intrinsic resistance [75, 89, 90]. It is therefore possible to say that *adeIJK* is the defining *Acinetobacter* pump, and to belong to the genus a species will encode a version of *adeIJK*. Important disease-causing *Acinetobacter* may also encode *adeABC*, which when overexpressed increases antibiotic resistance, such as in *A. baumannii* [8]. Therefore, it is advantageous in some species to have the combination of *adeIJK*, providing intrinsic resistance, and *adeABC*, synergistically providing even higher resistance. It is uncommon for *adeIJK* to be overexpressed, implying the functions it carries out are important and need to be tightly regulated [8, 23].

Funding information

E.M.D. is funded by the Wellcome Trust (222386/Z/21/Z),

Acknowledgements

The authors thank Massimiliano Lucidi for providing the cloning plasmid pVRL2 for this study, Ayush Kumar for providing *A. baumannii* ATCC 17978 Δ *adeAB* Δ *adeFGH* Δ *adeIJK* and Laura Piddock for providing *A. baumannii* ATCC 17978.

Author contribution

E.M.D. and J.M.A.B. conceptualized and designed the study. E.M.D. created the BLASTp database, and carried out genomic analyses and phenotypic work. V.N.B. provided protein modelling, analysis and discussion on structure. S.D. contributed to the Gubbins recombination analysis. The manuscript was written by E.M.D., J.M.A.B. and V.N.B., with input from A.M. and S.D.

Conflicts of interest

The authors declare that there are no conflicts of interest.

Ethical statement

This study did not require ethical approval.

References

- Baumann P. Isolation of *Acinetobacter* from soil and water. *J Bacteriol* 1968;96:39–42.
- Tacconelli E, Carrara E, Savoldi A, Harbarth S, Mendelson M, et al. Discovery, research, and development of new antibiotics: the WHO priority list of antibiotic-resistant bacteria and tuberculosis. *Lancet Infect Dis* 2018;18:318–327.
- Public Health England. Laboratory surveillance of *Acinetobacter* spp. bacteraemia in England, Wales and Northern Ireland: 2018; 2019. https://assets.publishing.service.gov.uk/government/uploads/system/uploads/attachment_data/file/810717/hpr2119_acntbctr.pdf
- Chusri S, Chongsuvivatwong V, Rivera JI, Silpapojakul K, Singkhamanan K, et al. Clinical outcomes of hospital-acquired infection with *Acinetobacter nosocomialis* and *Acinetobacter pittii*. *Antimicrob Agents Chemother* 2014;58:4172–4179.
- Kumar S, Patil PP, Singhal L, Ray P, Patil PB, et al. Molecular epidemiology of carbapenem-resistant *Acinetobacter baumannii* isolates reveals the emergence of *bla*OXA-23 and *bla*NDM-1 encoding international clones in India. *Infect Genet Evol* 2019;75:103986.
- Hamouda A, Amyes SGB. Novel *gyrA* and *parC* point mutations in two strains of *Acinetobacter baumannii* resistant to ciprofloxacin. *J Antimicrob Chemother* 2004;54:695–696.
- Coyne S, Rosenfeld N, Lambert T, Courvalin P, P erichon B. Overexpression of resistance-nodulation-cell division pump AdeFGH confers multidrug resistance in *Acinetobacter baumannii*. *Antimicrob Agents Chemother* 2010;54:4389–4393.
- Yoon E-J, Courvalin P, Grillo-Courvalin C. RND-type efflux pumps in multidrug-resistant clinical isolates of *Acinetobacter baumannii*: major role for AdeABC overexpression and AdeRS mutations. *Antimicrob Agents Chemother* 2013;57:2989–2995.
- Darby EM, Trampari E, Siasat P, Gaya MS, Alav I, et al. Molecular mechanisms of antibiotic resistance revisited. *Nat Rev Microbiol* 2022.
- Klenotic PA, Moseng MA, Morgan CE, Yu EW. Structural and functional diversity of resistance-nodulation-cell division transporters. *Chem Rev* 2021;121:5378–5416.
- Alav I, Kobylka J, Kuth MS, Pos KM, Picard M, et al. Structure, assembly, and function of tripartite efflux and type 1 secretion systems in Gram-negative bacteria. *Chem Rev* 2021;121:5479–5596.
- McNeil HE, Alav I, Torres RC, Rossiter AE, Laycock E, et al. Identification of binding residues between periplasmic adapter protein (PAP) and RND efflux pumps explains PAP-pump promiscuity and roles in antimicrobial resistance. *PLoS Pathog* 2019;15:e1008101.
- Chen M, Shi X, Yu Z, Fan G, Serysheva II, et al. In situ structure of the AcrAB-TolC efflux pump at subnanometer resolution. *Structure* 2022;30:107–113.
- Horiyama T, Yamaguchi A, Nishino K. TolC dependency of multidrug efflux systems in *Salmonella enterica* serovar Typhimurium. *J Antimicrob Chemother* 2010;65:1372–1376.

15. Seeger MA, Schiefner A, Eicher T, Verrey F, Diederichs K, et al. Structural asymmetry of AcrB trimer suggests a peristaltic pump mechanism. *Science* 2006;313:1295–1298.
16. Murakami S, Nakashima R, Yamashita E, Matsumoto T, Yamaguchi A. Crystal structures of a multidrug transporter reveal a functionally rotating mechanism. *Nature* 2006;443:173–179.
17. Nakashima R, Sakurai K, Yamasaki S, Hayashi K, Nagata C, et al. Structural basis for the inhibition of bacterial multidrug exporters. *Nature* 2013;500:102–106.
18. Nakashima R, Sakurai K, Yamasaki S, Nishino K, Yamaguchi A. Structures of the multidrug exporter AcrB reveal a proximal multi-site drug-binding pocket. *Nature* 2011;480:565–569.
19. Vargiu AV, Nikaïdo H. Multidrug binding properties of the AcrB efflux pump characterized by molecular dynamics simulations. *Proc Natl Acad Sci* 2012;109:20637–20642.
20. Magnet S, Courvalin P, Lambert T. Resistance-nodulation-cell division-type efflux pump involved in aminoglycoside resistance in *Acinetobacter baumannii* strain BM4454. *Antimicrob Agents Chemother* 2001;45:3375–3380.
21. Adams FG, Stroehner UH, Hassan KA, Marri S, Brown MH, et al. Resistance to pentamidine is mediated by AdeAB, regulated by AdeRS, and influenced by growth conditions in *Acinetobacter baumannii* ATCC 17978. *PLoS One* 2018;13:e0197412.
22. Chau S-L, Chu Y-W, Houang ETS. Novel resistance-nodulation-cell division efflux system AdeDE in *Acinetobacter* genomic DNA group 3. *Antimicrob Agents Chemother* 2004;48:4054–4055.
23. Damier-Piolle L, Magnet S, Brémont S, Lambert T, Courvalin P. AdelJK, a resistance-nodulation-cell division pump effluxing multiple antibiotics in *Acinetobacter baumannii*. *Antimicrob Agents Chemother* 2008;52:557–562.
24. Chu YW, Chau SL, Houang ETS. Presence of active efflux systems AdeABC, AdeDE and AdeXYZ in different *Acinetobacter* genomic DNA groups. *J Med Microbiol* 2006;55:477–478.
25. Williams CL, Neu HM, Gilbreath JJ, Michel SLJ, Zurawski DV, et al. Copper resistance of the emerging pathogen *Acinetobacter baumannii*. *Appl Environ Microbiol* 2016;82:6174–6188.
26. Srinivasan VB, Venkataramaiah M, Mondal A, Rajamohan G. Functional characterization of AbeD, an RND-type membrane transporter in antimicrobial resistance in *Acinetobacter baumannii*. *PLoS One* 2015;10:e0141314.
27. Tipton KA, Farokhyfar M, Rather PN. Multiple roles for a novel RND-type efflux system in *Acinetobacter baumannii* AB5075. *MicrobiologyOpen* 2017;6:e00418.
28. Subhadra B, Kim J, Kim DH, Woo K, Oh MH, et al. Local repressor AcrR regulates AcrAB efflux pump required for biofilm formation and virulence in *Acinetobacter nosocomialis*. *Front Cell Infect Microbiol* 2018;8:270.
29. Shi Y, Hua X, Xu Q, Yang Y, Zhang L, et al. Mechanism of eravacycline resistance in *Acinetobacter baumannii* mediated by a deletion mutation in the sensor kinase *adeS*, leading to elevated expression of the efflux pump AdeABC. *Infect Genet Evol* 2020;80:104185.
30. Lari AR, Ardebili A, Hashemi A. AdeR-AdeS mutations & overexpression of the AdeABC efflux system in ciprofloxacin-resistant *Acinetobacter baumannii* clinical isolates. *Indian J Med Res* 2018;147:413–421.
31. Fernando DM, Xu W, Loewen PC, Zhanel GG, Kumar A. Triclosan can select for an AdelJK-overexpressing mutant of *Acinetobacter baumannii* ATCC 17978 that displays reduced susceptibility to multiple antibiotics. *Antimicrob Agents Chemother* 2014;58:6424–6431.
32. Coyne S, Guigon G, Courvalin P, Périchon B. Screening and quantification of the expression of antibiotic resistance genes in *Acinetobacter baumannii* with a microarray. *Antimicrob Agents Chemother* 2010;54:333–340.
33. Lin L, Ling BD, Li XZ. Distribution of the multidrug efflux pump genes, *adeABC*, *adeDE* and *adelJK*, and class 1 integron genes in multiple-antimicrobial-resistant clinical isolates of *Acinetobacter baumannii*-*Acinetobacter calcoaceticus* complex. *Int J Antimicrob Agents* 2009;33:27–32.
34. Nemeš A, Maixnerová M, van der Reijden TJK, van den Broek PJ, Dijkshoorn L. Relationship between the AdeABC efflux system gene content, netilmicin susceptibility and multidrug resistance in a genotypically diverse collection of *Acinetobacter baumannii* strains. *J Antimicrob Chemother* 2007;60:483–489.
35. Katoh K, Standley DM. MAFFT multiple sequence alignment software version 7: improvements in performance and usability. *Mol Biol Evol* 2013;30:772–780.
36. National Centre for Biotechnology Information. BLAST: Basic Local Alignment Search Tool; 2021. <https://blast.ncbi.nlm.nih.gov/Blast.cgi>
37. Seemann T. Prokka: rapid prokaryotic genome annotation. *Bioinformatics* 2014;30:2068–2069.
38. Mikheenko A, Prjibelski A, Saveliev V, Antipov D, Gurevich A. Versatile genome assembly evaluation with QUAST-LG. *Bioinformatics* 2018;34:i142–i150.
39. Jain C, Rodriguez-R LM, Phillippy AM, Konstantinidis KT, Aluru S. High throughput ANI analysis of 90K prokaryotic genomes reveals clear species boundaries. *Nat Commun* 2018;9:5114.
40. Ondov BD, Treangen TJ, Melsted P, Mallonee AB, Bergman NH, et al. Mash: fast genome and metagenome distance estimation using MinHash. *Genome Biol* 2016;17:132.
41. Seeman T. ABRicate; 2020. <https://github.com/tseemann/abricate>
42. R Core Team. R: A language and environment for statistical computing. *R Foundation for Statistical Computing* 2017.
43. Wickham H. ggplot2: Elegant Graphics for Data Analysis; 2016. <https://ggplot2.tidyverse.org>
44. Yu G. Using ggtree to visualize data on tree-like structures. *Curr Protoc Bioinformatics* 2020;69:e96.
45. Wang L-G, Lam TT-Y, Xu S, Dai Z, Zhou L, et al. Treeio: an R package for phylogenetic tree input and output with richly annotated and associated data. *Mol Biol Evol* 2020;37:599–603.
46. Tonkin-Hill G, MacAlasdair N, Ruis C, Weimann A, Horesh G, et al. Producing polished prokaryotic pangenomes with the Panaroo pipeline. *Genome Biol* 2020;21:180.
47. Price MN, Dehal PS, Arkin AP. FastTree 2--approximately maximum-likelihood trees for large alignments. *PLoS One* 2010;5:e9490.
48. IBM Corp. *IBM SPSS Statistics for Macintosh*. Armonk, NY: IBM Corp; 2021.
49. Sullivan MJ, Petty NK, Beatson SA. Easyfig: a genome comparison visualizer. *Bioinformatics* 2011;27:1009–1010.
50. Croucher NJ, Page AJ, Connor TR, Delaney AJ, Keane JA, et al. Rapid phylogenetic analysis of large samples of recombinant bacterial whole genome sequences using Gubbins. *Nucleic Acids Res* 2015;43:e15.
51. Seeman T. Snippy; 2020. <https://github.com/tseemann/snippy>
52. Hadfield J, Croucher NJ, Goater RJ, Abudahab K, Aanensen DM, et al. Phandango: an interactive viewer for bacterial population genomics. *Bioinformatics* 2018;34:292–293.
53. Letunic I, Bork P. Interactive Tree Of Life (iTOL) v5: an online tool for phylogenetic tree display and annotation. *Nucleic Acids Res* 2021;49:W293–W296.
54. Zhang Z, Morgan CE, Bonomo RA, Yu EW, Projan SJ. Cryo-EM determination of eravacycline-bound structures of the ribosome and the multidrug efflux pump AdeJ of *Acinetobacter baumannii*. *mBio* 2021;12.
55. Yang J, Yan R, Roy A, Xu D, Poisson J, et al. The I-TASSER Suite: protein structure and function prediction. *Nat Methods* 2015;12:7–8.
56. Eicher T, Cha H, Seeger MA, Brandstätter L, El-Delik J, et al. Transport of drugs by the multidrug transporter AcrB involves an access and a deep binding pocket that are separated by a switch-loop. *Proc Natl Acad Sci* 2012;109:5687–5692.

57. Ornik-Cha A, Wilhelm J, Kobyłka J, Sjuts H, Vargiu AV, et al. Structural and functional analysis of the promiscuous AcrB and AdeB efflux pumps suggests different drug binding mechanisms. *Nat Commun* 2021;12:6919.
58. Lyu M, Moseng MA, Reimche JL, Holley CL, Dhulipala V, et al. Cryo-EM structures of a gonococcal multidrug efflux pump illuminate a mechanism of drug recognition and resistance. *mBio* 2020;11:e00996-20.
59. Robert X, Gouet P. Deciphering key features in protein structures with the new ENDScript server. *Nucleic Acids Res* 2014;42:W320-4.
60. Lucidi M, Runci F, Rampioni G, Frangipani E, Leoni L, et al. New shuttle vectors for gene cloning and expression in multidrug-resistant *Acinetobacter* species. *Antimicrob Agents Chemother* 2018;62.
61. Wijers CDM, Pham L, Menon S, Boyd KL, Noel HR, et al. Identification of two variants of *Acinetobacter baumannii* strain ATCC 17978 with distinct genotypes and phenotypes. *Infect Immun* 2021;89:e0045421.
62. Sambrook J, Russell DW. Transformation of *E. coli* by electroporation. *CSH Protoc* 2006;2006:pdb.prot3933.
63. Plasmidsaurus. Plasmidsaurus Sequencing; (n.d.). <https://www.plasmidsaurus.com/>
64. CLSI. *Performance Standards for Antimicrobial Susceptibility Testing*. 31st ed. 2020.
65. Andrews JM. Determination of minimum inhibitory concentrations. *J Antimicrob Chemother* 2001;48 Suppl 1:5-16.
66. Hagman KE, Lucas CE, Balthazar JT, Snyder L, Nilles M, et al. The MtrD protein of *Neisseria gonorrhoeae* is a member of the resistance/nodulation/division protein family constituting part of an efflux system. *Microbiology* 1997;143:2117-2125.
67. Coyne S, Courvalin P, Périchon B. Efflux-mediated antibiotic resistance in *Acinetobacter* spp. *Antimicrob Agents Chemother* 2011;55:947-953.
68. Roca I, Espinal P, Martí S, Vila J. First identification and characterization of an AdeABC-like efflux pump in *Acinetobacter* genomospecies 13TU. *Antimicrob Agents Chemother* 2011;55:1285-1286.
69. Morgan CE, Glaza P, Leus IV, Trinh A, Su C-C, et al. Cryoelectron microscopy structures of AdeB illuminate mechanisms of simultaneous binding and exporting of substrates. *mBio* 2021;12:1-15.
70. Tam HK, Foong WE, Oswald C, Herrmann A, Zeng H, et al. Allosteric drug transport mechanism of multidrug transporter AcrB. *Nat Commun* 2021;12:3889.
71. Su C-C, Morgan CE, Kambakam S, Rajavel M, Scott H, et al. Cryoelectron microscopy structure of an *Acinetobacter baumannii* multidrug efflux pump. *mBio* 2019;10:e01295-19.
72. Murakami S, Nakashima R, Yamashita E, Yamaguchi A. Crystal structure of bacterial multidrug efflux transporter AcrB. *Nature* 2002;419:587-593.
73. Johnson RM, Fais C, Parmar M, Cheruvara H, Marshall RL, et al. Cryo-EM structure and molecular dynamics analysis of the fluoroquinolone resistant mutant of the AcrB transporter from *Salmonella*. *Microorganisms* 2020;8:943.
74. Morgan CE, Zhang Z, Bonomo RA, Yu EW. An analysis of the novel fluoroquinolone TP-6076 bound to both the ribosome and multidrug efflux pump AdeJ from *Acinetobacter baumannii*. *mBio* 2022;13:e0373221.
75. Yoon E-J, Balloy V, Fiette L, Chignard M, Courvalin P, et al. Contribution of the Ade resistance-nodulation-cell division-type efflux pumps to fitness and pathogenesis of *Acinetobacter baumannii*. *mBio* 2016;7:e00697-16.
76. Jerse AE, Sharma ND, Simms AN, Crow ET, Snyder LA, et al. A gonococcal efflux pump system enhances bacterial survival in a female mouse model of genital tract infection. *Infect Immun* 2003;71:5576-5582.
77. Buckley AM, Webber MA, Cooles S, Randall LP, La Razione RM, et al. The AcrAB-TolC efflux system of *Salmonella enterica* serovar Typhimurium plays a role in pathogenesis. *Cell Microbiol* 2006;8:847-856.
78. Hirakata Y, Srikumar R, Poole K, Gotoh N, Suematsu T, et al. Multi-drug efflux systems play an important role in the invasiveness of *Pseudomonas aeruginosa*. *J Exp Med* 2002;196:109-118.
79. Lin J, Sahin O, Michel LO, Zhang Q. Critical role of multidrug efflux pump CmeABC in bile resistance and in vivo colonization of *Campylobacter jejuni*. *Infect Immun* 2003;71:4250-4259.
80. Bina XR, Provenzano D, Nguyen N, Bina JE. *Vibrio cholerae* RND family efflux systems are required for antimicrobial resistance, optimal virulence factor production, and colonization of the infant mouse small intestine. *Infect Immun* 2008;76:3595-3605.
81. Kornelsen V, Kumar A. Update on multidrug resistance efflux pumps in *Acinetobacter* spp. *Antimicrob Agents Chemother* 2021;65:e0051421.
82. Sugawara E, Nikaido H. Properties of AdeABC and AdeJK efflux systems of *Acinetobacter baumannii* compared with those of the AcrAB-TolC system of *Escherichia coli*. *Antimicrob Agents Chemother* 2014;58:7250-7257.
83. Zwama M, Yamasaki S, Nakashima R, Sakurai K, Nishino K, et al. Multiple entry pathways within the efflux transporter AcrB contribute to multidrug recognition. *Nat Commun* 2018;9:124.
84. Sennhauser G, Bukowska MA, Briand C, Grütter MG. Crystal structure of the multidrug exporter MexB from *Pseudomonas aeruginosa*. *J Mol Biol* 2009;389:134-145.
85. Zwama M, Nishino K. Proximal Binding Pocket Arg717 Substitutions in *Escherichia coli* AcrB Cause Clinically Relevant Divergencies in Resistance Profiles. *Antimicrobial agents and chemotherapy* 2022;66:e02392-21.
86. Chitsaz M, Booth L, Blyth MT, O'Mara ML, Brown MH. Multidrug Resistance in *Neisseria gonorrhoeae*: Identification of Functionally Important Residues in the MtrD Efflux Protein. *mBio* 2019;10:e02277-19.
87. Hernández-González IL, Mateo-Estrada V, Castillo-Ramírez S. The promiscuous and highly mobile resistome of *Acinetobacter baumannii*. *Microb Genom* 2022;8:000762.
88. Naidu V, Bartczak A, Brzoska AJ, Lewis P, Eijkelkamp BA, et al. Evolution of RND efflux pumps in the development of a successful pathogen. *Drug Resist Updat* 2023;66:100911.
89. Yoon E-J, Chabane YN, Goussard S, Snesrud E, Courvalin P, et al. Contribution of resistance-nodulation-cell division efflux systems to antibiotic resistance and biofilm formation in *Acinetobacter baumannii*. *mBio* 2015;6:e00309-15.
90. Knight DB, Rudin SD, Bonomo RA, Rather PN. *Acinetobacter nosocomialis*: defining the role of efflux pumps in resistance to antimicrobial therapy, surface motility, and biofilm formation. *Front Microbiol* 2018;9:1902.
91. Anes J, McCusker MP, Fanning S, Martins M. The ins and outs of RND efflux pumps in *Escherichia coli*. *Front Microbiol* 2015;6:587.
92. Zwama M, Yamaguchi A, Nishino K. Phylogenetic and functional characterisation of the *Haemophilus influenzae* multidrug efflux pump AcrB. *Commun Biol* 2019;2:340.
93. Zulfiqar S, Shakoori AR. Molecular characterization, metal uptake and copper induced transcriptional activation of efflux determinants in copper resistant isolates of *Klebsiella pneumoniae*. *Gene* 2012;510:32-38.
94. Ni RT, Onishi M, Mizusawa M, Kitagawa R, Kishino T, et al. The role of RND-type efflux pumps in multidrug-resistant mutants of *Klebsiella pneumoniae*. *Sci Rep* 2020;10:10876.
95. Pasqua M, Grossi M, Scinicariello S, Aussel L, Barras F, et al. The MFS efflux pump EmrKY contributes to the survival of *Shigella* within macrophages. *Sci Rep* 2019;9:2906.
96. Stothard P. The sequence manipulation suite: JavaScript programs for analyzing and formatting protein and DNA sequences. *Biotechniques* 2000;28:1102, 1104.